Available online at www.sciencedirect.com
SCIENCE DIRECT®
Thermochimica Acta 420 (2004) 127–134
thermochimica acta
www.elsevier.com/locate/tca

Calorimetric determination of the acidic character of amorphous and crystalline aluminosilicates

Brindusa Dragoi [a,b], Antonella Gervasini [c], Emil Dumitriu [b], Aline Auroux [a,*]

[a] *Institut de Recherches sur la Catalyse, CNRS, 2 Av. Einstein, 69626 Villeurbanne, Cedex, France*
[b] *Laborator Cataliza, Facultatea de Chimie Industriala, Universitatea Tehnica "Gh. Asachi", 71A Bd. D. Mangeron, 6600 Iasi, Romania*
[c] *Dipartimento di Chimica Fisica ed Elettrochimica, Università di Milano, via C. Golgi, 19, 20133 Milan, Italy*

Received 29 July 2003; accepted 22 October 2003
Available online 27 July 2004

Abstract

Aluminosilicates can present different structures such as crystalline true zeolite molecular sieves or amorphous silica–aluminas. With a large surface area available, both can be involved as catalysts, adsorbents or catalyst supports, and the determination of their surface acidic properties is an important parameter in the study of such materials.

The number, strength and strength distribution of the acidic sites were determined using microcalorimetry linked to a volumetric line. Ammonia was used as a basic probe molecule. The adsorption temperatures ranged from 353 K up to 473 K. The samples consisted of two amorphous silica–aluminas (Si/Al ≈ 6.5) and three microporous zeolites H-β, H-ZSM-5 and H-MCM-22 with similar Si/Al ratios (Si/Al ≈ 13).

The differential heats of ammonia adsorption versus coverage and the corresponding isotherms are given. The H-ZSM-5, H-MCM-22, H-β samples display a plateau of constant adsorption heats near 150 kJ mol^{-1}, while the silica–alumina samples present continuously decreasing heats from 150 kJ mol^{-1} at zero coverage to 40 kJ mol^{-1} at high coverage, due to their surface heterogeneity. For amorphous silica–aluminas, the number of acid sites is dependent of the aluminum distribution at the surface.

The differences observed in the adsorption behavior of ammonia over the three zeolites arise from differences in their morphology, i.e. the total free volumes, pore geometries and electric field gradients at the adsorption sites. The adsorption isosteres have also been calculated from the adsorption isotherms, and the isosteric heats of adsorption have been compared with the heats measured by calorimetry.

Keywords: Silica–aluminas; Zeolites; Microcalorimetry; Acidity

1. Introduction

It is already known that one of the most important applications of silica is as catalyst support or host oxide. Silica by itself has no activity and very little acidity. However, Gayer [1], in 1933, was the first to note that the introduction of small amounts of alumina induces an increase in both the activity and the acidity of the mixture [2]. Silica is also known to stabilize the alumina surface and form tetrahedrally coordinated silica–alumina species on the alumina surface to produce Brönsted acidity [3].

So, in order to obtain improved surface properties and in particular stronger acidic sites, the structure of silica has been modified with alumina, leading to new types of materials named aluminosilicates. Although each of the components (SiO_2, Al_2O_3) serves a specific purpose in the catalyst particle, they often interact synergistically. Moreover the catalyst architecture plays a fundamental role.

Aluminosilicates can be divided into two categories, amorphous silica–aluminas and crystalline zeolite molecular sieves.

For example, amorphous silica–alumina, in which aluminum is tetrahedrally coordinated to silicon through oxygen bridges, was the active cracking component in many FCC catalysts before the discovery of zeolites.

In crystalline aluminosilicates, all aluminum and silicon atoms form tetrahedra which are linked by shared oxygen

* Corresponding author. Tel.: +33 472 44 53 98; fax: +33 472 44 53 99.
E-mail address: auroux@catalyse.cnrs.fr (A. Auroux).

0040-6031/$ – see front matter © 2004 Elsevier B.V. All rights reserved.
doi:10.1016/j.tca.2003.10.031

atoms. These tetrahedra join with each other to form secondary building units, which can be interconnected to give numerous distinctive zeolite structures. Each has a regular and well defined pore structure together with inner cavities. This precise control of pore size is one of the greatest distinctions between zeolites and amorphous silica–aluminas [2].

The aim of this work was to compare the acidic character of these two kinds of materials using the adsorption microcalorimetry technique, which gives access to the number, strength and strength distribution of the acid sites [4].

2. Experimental

Besides a classical silica (Aerosil) five samples were considered: two amorphous silica–aluminas (SiO_2–Al_2O_3) named SAH and SAG, and three crystalline microporous zeolites presenting various structural geometries: H-ZSM-5, H-BETA and H-MCM-22.

2.1. Preparation of catalysts

2.1.1. Preparation of amorphous silica–aluminas

The synthesis of the amorphous silica–alumina SAH was carried out by a sol–gel method using tetraethylorthosilicate (TEOS; $Si(OC_2H_5)_4$; Fluka), aluminum isopropoxide ($Al(i\text{-}OC_3H_7)_3$, Fluka, 97% purity), absolute ethanol, tetrapropylammonium hydroxide (TPAOH, $(CH_3CH_2CH_2)_4NOH$, Fluka), deionized water. This method, which implies two steps, hydrolysis and then hydroxyl condensation, has already been reported in the literature by Perego et al. [5]. Aluminum isopropoxide, TPAOH and deionized water were introduced into a reactor with three necks, equipped with magnetic stirring and thermostated up to 333 K, forming a homogenous suspension. Ethanol and TEOS were added to this solution, and after approximately 10 min. a compact and opal gel was obtained. This gel was then subjected to maturing for 18 h at room temperature, followed by drying at 393 K for 6 h and finally calcination at 823 K for 8 h. The second silica–alumina (SAG) was supplied by Grace Catalysts & Carriers. The preparation mode is not given by the supplier but the sample resembles to a silica coated alumina.

2.1.2. Preparation of zeolites

The MCM-22 zeolite was hydrothermally synthesized using hexamethylenimine (HMI, $C_7H_{13}N$, 99% purity, Aldrich) as organic template, SiO_2 (Aerosil-200, Degussa), sodium aluminate ($NaAlO_2$; 56% Al_2O_3, 37% Na_2O, Carlo Erba), sodium hydroxide (NaOH 98% purity, Prolabo) and deionized water. This zeolite was prepared according to the method previously reported in the literature [6].

The general procedure of synthesis is as follows. Sodium aluminate and sodium hydroxide were dissolved in deionized water. Then, HMI was added to this solution under stirring. After 10 min. silica was added with vigorous stirring that was maintained for 30 min. The resulting gel was introduced into a Teflon-lined stainless autoclave and heated at 423 K for 7 days in dynamic conditions (60 rpm). After cooling the autoclave in cold water, the sample was filtered and washed with deionized water until a pH around 9.0 was obtained. Then, the synthesized material was calcined in air at 823 K for 12 h in order to remove the organic template from the zeolite pores.

The HZSM-5 zeolite was supplied by Degussa and the H-BETA zeolite by Rhône-Poulenc.

2.2. Characterization

X-ray diffraction measurements were performed on a Bruker D5005 apparatus between 3 and 80° (2θ) using Cu Kα radiation ($\lambda = 1.54184$ Å).

The BET surface areas (S_{BET}) were determined by nitrogen adsorption at 77 K after pretreatment for 4.0 h at 673 K under vacuum.

The calorimetric experiments were carried out in a microcalorimeter of Tian–Calvet type (C80 from Setaram) linked to a volumetric line that makes it possible to study the gas–solid interactions [4]. This type of microcalorimeter usually employs two cells, one containing the adsorbent and the other an empty reference cell. The adsorption takes place by repeatedly sending small doses of gas onto the initially outgassed solid while recording the heat flow signal and the concomitant pressure evolution. The adsorption temperature is maintained at a constant value (usually of the order of 423 K, in order to limit physisorption).

In this study, NH_3 was chosen as basic probe molecule because of its small diameter (0.3 nm) and strong basicity ($pK_a = 9.25$; proton affinity $= 858\ kJ\ mol^{-1}$). The samples were pretreated under vacuum at 673 K overnight. NH_3 adsorption was performed at three different temperatures (353 K, 423 K, 473 K). The equilibrium pressure was measured after each dose by a Barocel Capacitance Manometer (Datametrics).

The irreversibly chemisorbed amount can be evaluated from the difference between the primary adsorption isotherm (adsorbed volume as a function of equilibrium pressure over the sample) and the secondary isotherm obtained after desorption under vacuum and readsorption of the basic probe at the same temperature. This difference can be roughly interpreted as the amount of strong sites (often associated with adsorption heats at least of the order of 100–150 $kJ\ mol^{-1}$).

3. Results and discussion

The physicochemical characteristics of the samples are listed in Table 1 which gives the Si/Al ratio (from chemical analysis), BET surface area and pore diameter for each sample.

Table 1
Structural aspects of studied samples

Sample	IZA code	Si/Al molar ratio (CA)	Surface area ($m^2\,g^{-1}$)	Average pore diameter (nm)
SiO_2–Al_2O_3 (SAH)		6.5	777	3.5
SiO_2–Al_2O_3 (SAG)		6.0	485	n.d.
H-MCM-22	MWW	12.5	447	0.40 × 0.55[a] | 0.41 × 0.51[a,b]
H-ZSM-5	MFI	14	367	{0.53 × 0.56 – 0.51 × 0.55}[b,c]
H-BETA	BEA	12.5	633	0.64 × 0.67[a] – 0.56 × 0.56[b,d]

(–) intersecting channels; (|) non-intersecting channels.
[a] Two-dimensional channels.
[b] Atlas of zeolite framework types [7].
[c] Three-dimensional channels.
[d] Monodimensional channels.

The samples investigated consist of two amorphous materials which present similar Si/Al ratios (around 6.5) but different surface areas, and three zeolite structures with almost the same Si/Al ratio (≈13 from chemical analysis) and different surface areas. As a result of silica structure modification, the surface area of the amorphous materials was increased from around $300\,m^2\,g^{-1}$ for pure silica up to $777\,m^2\,g^{-1}$ (SiO_2–Al_2O_3; SAH) and $485\,m^2\,g^{-1}$ (SiO_2–Al_2O_3; SAG). In microporous materials the adsorbed N_2 molecules fill the pores completely and, because of the limited space, multilayer adsorption is suppressed. Therefore, the BET surface area, meaningless, can only be used as a purely empirical value to compare the quality and porosity of materials of the same kind [8]. Concerning pore diameter, amorphous materials can be classified as mesoporous, while the studied zeolites are microporous (pore size below 2 nm).

Fig. 1 shows the powder XRD patterns of the three zeolites ZSM-5, MCM-22, BETA, as well as a pattern characteristic of an amorphous silica–alumina (SAH). As expected, for the amorphous materials there were no peaks in the XRD spectra. Crystalline materials have peaks at values of 2θ which, together with the peak intensities, are characteristic of the structure of the material.

The studied zeolites present different morphologies. The structure of MCM-22 consists of layers linked together along the *c*-axis by oxygen bridges. The particular architecture of this material includes two channel systems with different pore dimensions. One of these pore systems is formed of two-dimensional 10 MR (10-membered rings) sinusoidal channels whereas the second one presents large supercages defined by 12 MR, also accessed through 10 MR openings [9–11].

ZSM-5 has only 10 MR pore openings. The particularity of the ZSM-5 framework resides in the fact that it has two intersecting channel systems, one of them sinusoidal and the other one straight [12,13]. This structure gives rise to better catalytic properties and higher thermal stability.

Different from the first two zeolites, BETA zeolite possesses a peculiar structure, disorganized in the *c*-direction [14]. The framework is formed by two kinds of intersecting channels which have 12 MR pore openings. All BETA zeolite materials synthesized to this date show extreme structural disorder.

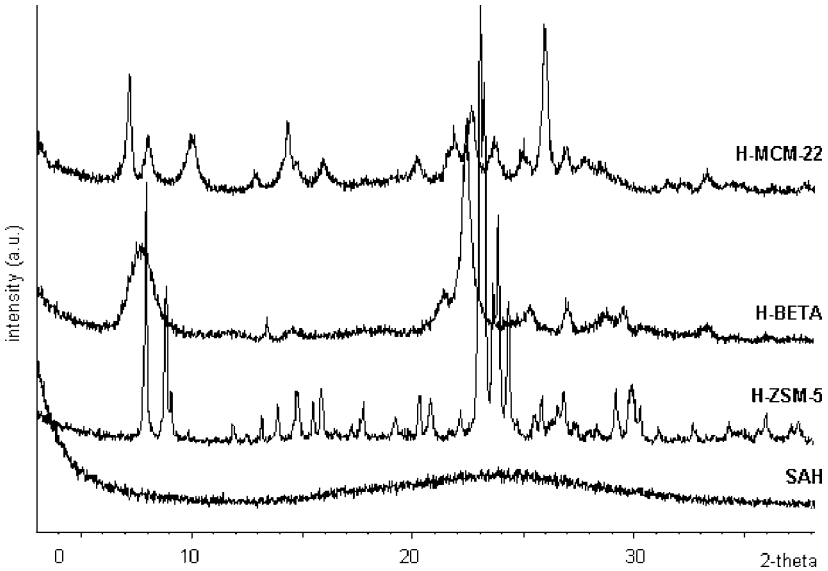

Fig. 1. X-ray diffraction patterns of SiO_2–Al_2O_3, H-ZSM-5, H-BETA and H-MCM-22.

The framework composition affects the stability of a material. For example a high silica zeolite usually has a higher thermal stability than the corresponding aluminosilicate. The channels and cages of a zeolite framework are usually filled with extra-framework species such as exchangeable cations, which balance the negative charge of the framework [14].

All these materials present different acidic properties depending of the manner in which aluminum was incorporated in the structure.

Synthetic silica–alumina materials are amorphous in nature, their structure consisting of a random array of silica and alumina tetrahedra interconnected over three dimensions. When forced into a tetrahedral configuration via oxygen bridges, an aluminum atom develops a negative charge, and the resultant compensating cations are the source of the acid sites. Hence, the surface defects are the main source of acidity [2].

Improved catalytic performance is usually observed for well-structured materials like zeolites; this has been reported for example in the case of *n*-hexane cracking when comparing an amorphous silica–alumina to a zeolite ordered system [15]. The catalytic activity of molecular sieves is affected by the type of acid sites available (Brönsted or Lewis), the concentration of those sites and their strength. Important factors related to the acid site configuration are: the number of acid sites, their strength, and their distribution in the lattice. The active sites of aluminosilicate zeolites are complex and comprise of hydroxyl groups bridging Si and Al atoms, which have strong Brönsted acid properties, and oxo bridges, which have Lewis base properties. For materials like H-ZSM-5 the concentration of Brönsted sites is approximately equal to the framework Al content. Factors influencing the acid properties of zeolites include the method of preparation, the temperature of dehydration, the Si/Al ratio, and the distribution of the framework atoms.

Finding a simple correlation between the number, type and strength of the acid sites in aluminosilicate materials and their catalytic activity is the ultimate goal. While such a goal has yet to be fully achieved, considerable advances have been made in the area of quantifying the number and strength of the active acid sites by using adsorption microcalorimetry of basic probe molecules.

Fig. 2 represents differential heats of NH_3 adsorption versus coverage, measured at 353 K, 423 K and 473 K for each studied structure, while Fig. 3 reports the differential heats of ammonia adsorption for all samples at the same temperature (473 K).

Typically, the differential heat of adsorption, defined as the heat evolved during the adsorption of a small quantity of gas a constant temperature, is determined as a function of the surface coverage. The heat of adsorption of a basic molecule on an acidic site is claimed to be characteristic of the strength of the site. To obtain an acid strength distribution from the heat of adsorption as a function of coverage, the sample temperature has to be sufficiently high to assure that the probe molecule reaches the sorption equilibrium on the sites being probed [8].

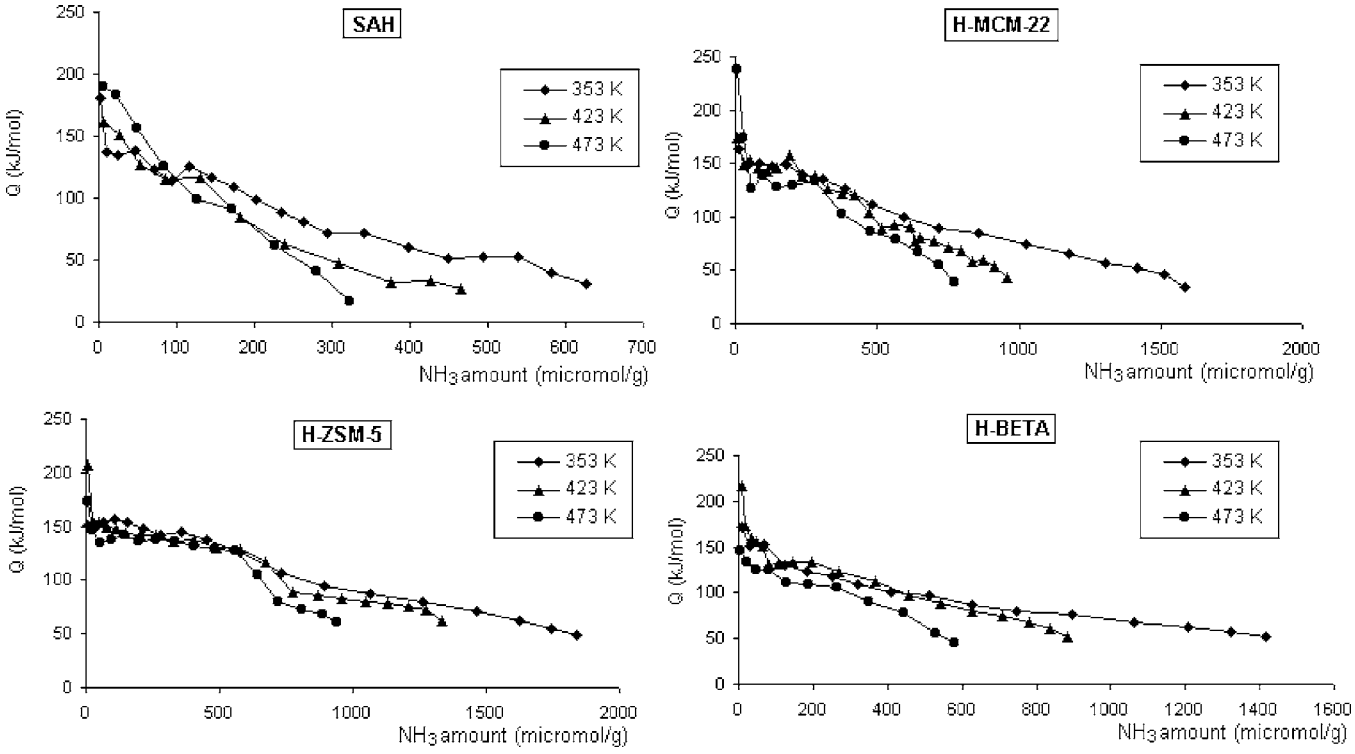

Fig. 2. Differential heats of NH_3 adsorption at three different temperatures for SAH, H-MCM-22, H-ZSM-5 and H-BETA vs. NH_3 amounts adsorbed.

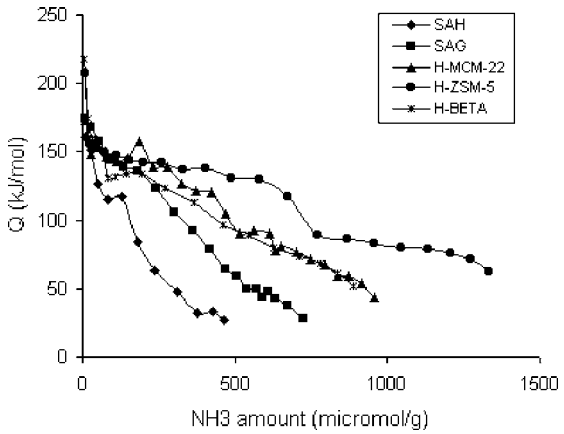

Fig. 3. Differential heats of NH_3 adsorption vs. coverage at 423 K for all samples.

The dependence of the heat of adsorption on the coverage provides detailed information on the interaction of the probe molecule with the zeolite. A typical differential heat plot shows three regions in the case of a zeolite. The sharp decrease of Q_{diff} at low coverage indicates the presence of a small concentration of very strong Lewis type acid sites. The plateau of constant heats of adsorption that follows results from the adsorption of NH_3 on the Brönsted-type acid sites. The differential heat then decreases sharply after all Brönsted-type acid sites are covered. For the adsorption of NH_3 on Al^{3+} cations only, the heat of adsorption is lower and decreases continuously with coverage [8].

As a general view, it can be seen that the differential heats of adsorption versus the amount of ammonia adsorbed present a continuously decreasing profile for silica–alumina (SAH), while for ordered materials, the differential heats present a more or less narrow plateau near 150 kJ mol^{-1}. This plateau is more visible for ZSM-5 than for the other zeolites.

Both Brönsted and Lewis type acid sites are present in zeolites. Brönsted acidity is due primarily to acidic hydroxyl groups attached to the framework, while Lewis acidity is attributed mostly to non-framework aluminum species. The application of ^{29}Si NMR provides direct information on the composition and Si/Al distribution of the tetrahedral framework, independently of the presence of non-framework Al species. In our ZSM-5 zeolite the number of acidic hydroxyl groups attached to the framework is equivalent to the number of framework aluminum atoms, as this sample presents very few EFAL (extra-framework aluminum) species (the Si/Al ratio as determined by the ^{29}Si and ^{27}Al MAS NMR spectra is around 18 and very close to the Si/Al ratio provided by chemical analysis). This is not the case for the BETA zeolite, which presents many EFAL species (global Si/Al = 12.5 while the framework Si/Al is equal to 45 from MAS NMR).

For each sample (except for SAG, not given), Fig. 2 provides three differential heat curves, corresponding to the three different adsorption temperatures investigated. The shape of these differential heat curves suggests a variation in the selectivity of adsorption at different temperatures, namely that adsorption occurs on stronger acid sites, rather than on the weaker or non-acidic sites at higher temperatures, while at lower temperatures all kinds of centers are involved in the adsorption process. In fact, the measured heats of adsorption are indicative of the surface homogeneity or heterogeneity in terms of energy distribution [16,17], as shown by our experiments.

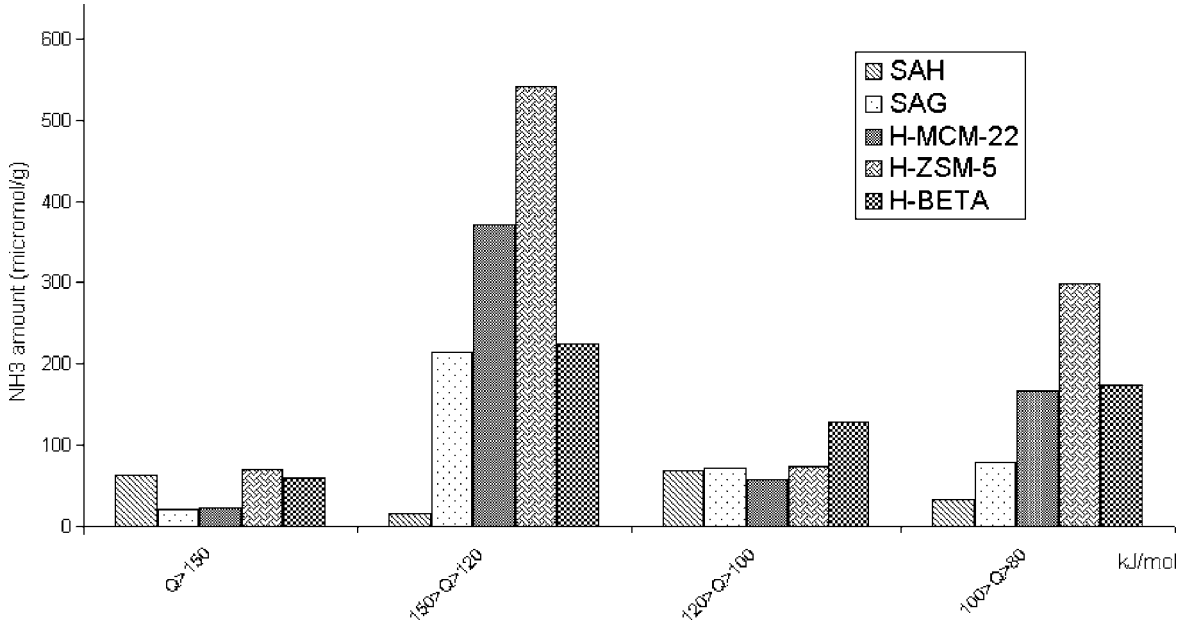

Fig. 4. Acidic strength distribution of the samples.

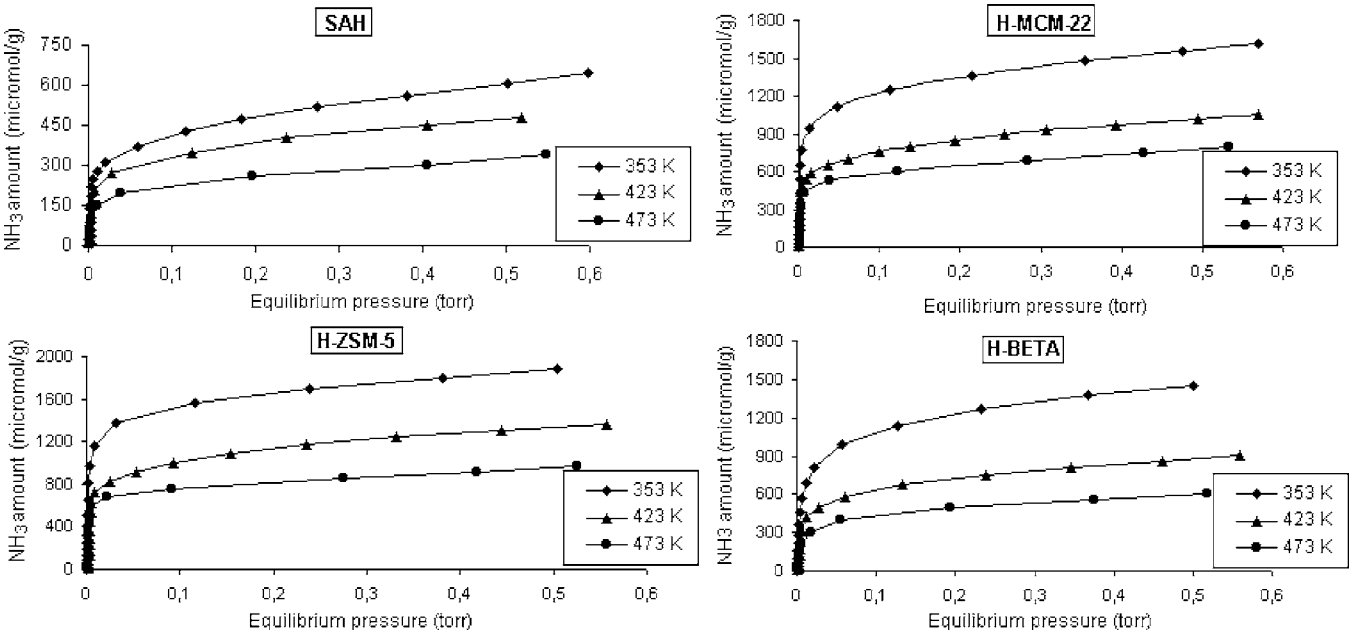

Fig. 5. Volumetric adsorption isotherms at three different temperatures for the studied samples.

Fig. 4 represents the number of sites in a given strength range calculated from differential heats of ammonia adsorption. It can be seen that for all samples the main population of strongly acidic sites gives rise to adsorption heats between 150 and 120 kJ mol^{-1}. In addition, for SAG the number of the acid sites in the above-mentioned interval is comparable with one of the zeolite structures (H-BETA). Since this is an amorphous material, we can explain this behavior by the presence of more defects on the surface of SAG than for SAH. In comparison, pure silica gives rise to very low adsorption heats (∼40 kJ mol^{-1}).

The volumetric isotherms (number of adsorbed molecules n as a function of the equilibrium pressure p) represented in Fig. 5 consist of two distinct parts. The vertical part can be assigned to irreversible adsorption, namely chemisorption, while the horizontal part corresponds to reversible adsorption (physisorption).

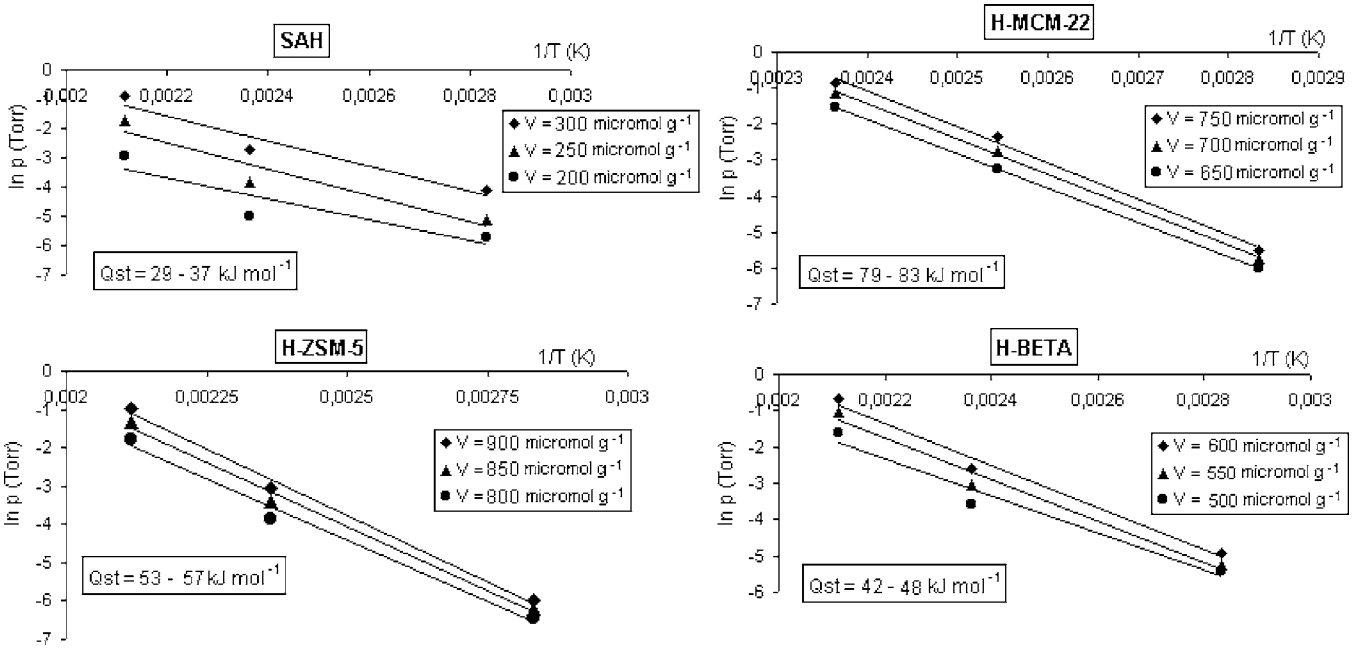

Fig. 6. Adsorption isosteres and isosteric heats for the studied samples.

Table 2
Acidic properties of the samples

Sample	Total number of acid sites (μmol g^{-1})	Number of strong acid sites (μmol g^{-1})	Integral heat (J g^{-1})	Average heat (kJ mol^{-1})	Isosteric heat (kJ mol^{-1})
SAH	386	219	35	89	33
SAG	621	400	64	104	54
H-MCM-22	855	495	97	115	81
H-ZSM-5	1137	720	134	118	55
H-BETA	720	438	81	112	45

These curves show that, at low pressures (up to 0.01 torr), chemisorption is the predominant process, and that physisorption begins above this value. This behavior is normal because chemisorption concerns only a limited number of sites, namely the stronger sites, whereas reversible adsorption can occur on all types of centers.

On the other hand and in agreement with the Van't Hoff law, the adsorption of NH_3 is less favored at higher temperatures, as shown by the experimental isotherms. Accordingly, the Henry zone is diminished at higher temperatures.

From the experimental isotherms we can plot the corresponding isosteres (Fig. 6) for surface coverages that are included in the physical adsorption range of the isotherms, namely between 200–300 μmol g^{-1}, 500–600 μmol g^{-1}, 650–750 μmol g^{-1} and 800–900 μmol g^{-1} for SiO_2–Al_2O_3 (SAH), H-BETA, H-MCM-22 and H-ZSM-5, respectively.

The adsorption isosteres were obtained by plotting ln(p) versus 1/T. From the slopes of these lines, isosteric heats of adsorption, Q_{st} were evaluated in agreement with the Clausius–Clapeyron equation [18,19]:

$$Q_{st} = -RZ\left(\frac{\partial \ln p}{\partial(1/T)}\right)_n$$

where p and T denote, respectively, the equilibrium pressure and absolute temperature, R is the universal gas constant, Z is the compressibility coefficient (with $Z = 1$ for an ideal gas phase), and n is the adsorbate coverage.

Higher values of Q_{st} were obtained for the zeolite samples (81 kJ mol^{-1} for H-MCM-22, 55 kJ mol^{-1} for H-ZSM-5, and 45 kJ mol^{-1} for H-BETA) than for the amorphous silica–alumina SAH (33 kJ mol^{-1} for SAH, compared to 54 kJ mol^{-1} for SAG).

The differential and isosteric heats of adsorption are in principle related by the relation $Q_{st} = Q_{diff} + ZRT$ [20]. The Q_{st} values that we obtained are always smaller than the corresponding differential heats at the same coverage level, but the accuracy on the determination of the slope of the isosteres is relatively low at such low equilibrium pressure. In fact, the equations presented above are based on the assumptions that the adsorption is reversible, that the partial molar volume of the gas is much greater than that of the adsorbate, that the gas behaves ideally, that the surface state is invariable during measurement, and that the heat does not change with changes in temperature [21].

Table 2 summarizes the acidity measurement results obtained from adsorption calorimetry at 423 K by giving the total number of acid sites (in μmol NH_3 per gram of sample) at the given equilibrium pressure of 0.2 torr, the number of strong acid sites (derived from the irreversibly adsorbed NH_3 volume), the integral heat at 0.2 torr (in J g^{-1}), the average differential heat (integral heat divided by NH_3 uptake) over the 0–0.2 torr range, and the calculated isosteric heat. The following order of acidity (both in number and strength of acid sites) can be given:

$$\text{H-ZSM-5} > \text{H-MCM-22} > \text{H-BETA} > \text{SAG} > \text{SAH} \gg SiO_2.$$

4. Conclusion

The calorimetric studies have shown that the acidity of the alumina-modified silica structures is dependent on the "order degree" of the structure. Thus, amorphous silica–aluminas contain a smaller number of acid sites than crystalline molecular sieves; the acid strength in terms of heat evolved is also more important for ordered materials.

For amorphous silica–aluminas, the surface acid sites are heterogeneous (no plateau of differential heats); the number of these sites depends on the aluminum distribution on the surface, and the acid strength depends on the structural defects of the surface (more important for SAG than for SAH). For crystalline zeolites, the surface acid sites are more homogeneous, with the presence of a plateau of adsorption heats; the acid strength is higher than for amorphous samples, and the number and strength of the acid sites depend on the location of aluminum species (presence of EFAL).

References

[1] F.H. Gayer, Ind. Eng. Chem. 25 (1933) 1122.
[2] A. Humphries, D.H. Harris, P. O'Connor, in: J.S. Magee, M.M. Mitchell Jr. (Eds.), Fluid Catalytic Cracking: Science and Technology, Elsevier, Stud. Surf. Sci. Catal. 76 (1993) 41.
[3] G.M. Woltermann, J.S. Magee, S.D. Griffith, in: J.S. Magee, M.M. Mitchell Jr. (Eds.), Fluid Catalytic Cracking: Science and Technology, Elsevier, Stud. Surf. Sci. Catal. 76 (1993) 105.
[4] A. Auroux, Top. Catal. 4 (1997) 71; 19 (2002) 205.
[5] C. Perego, S. Amrarilli, A. Carati, C. Flego, G. Pazzucconi, C. Rizzo, G. Bellussi, Microporous Mesoporous Mater. 27 (1999) 345.
[6] A. Corma, C. Corell, J. Pérez-Pariente, Zeolites 15 (1995) 2.
[7] C. Baerlocher, W.M. Meier, D.H. Olson, Atlas of Zeolite Framework Types, fifth ed., Elsevier, Amsterdam, 2001.

[8] A. Jentis, J.A. Lercher, in: H. Van Bekkum, E.M. Flamingen, P.A. Jacobs, J.C. Jansen (Eds.), Introduction to Zeolite Science and Practice, Elsevier, Stud. Surf. Sci. Catal. 137 (2001) 345.
[9] M.E. Leonowicz, J.A. Lawton, S.L. Lawton, M.K. Rubin, Science 264 (1994) 1817.
[10] G.J. Gopalakrishnan, L.F. Raul, Microporous Mesoporous Mater. 40 (2000) 9.
[11] A. Corma, C. Corell, J. Pérez-Pariente, J.M. Guil, R. Guil-Lopez, S. Nicolopoulos, J. Gonzalez Calbet, M. Vallet-Regi, Zeolites 16 (1996) 7.
[12] S. Bhatia, Zeolite Catalysis: Principles and Applications, CRC Press, Inc., Boca Raton, FL, 1990.
[13] P.A. Jacobs, H.K. Beyer, J. Valyon, Zeolites 1 (1981) 161.
[14] L.B. McCusker, C. Baerlocher, in: H. Van Bekkum, E.M. Flamingen, P.A. Jacobs, J.C. Jansen (Eds.), Introduction to Zeolite Science and Practice, Elsevier, Stud. Surf. Sci. Catal. 137 (2001) 37.
[15] R. Szostak, in: H. Van Bekkum, E.M. Flamingen, P.A. Jacobs, J.C. Jansen (Eds.), Introduction to Zeolite Science and Practice, Elsevier, Stud. Surf. Sci. Catal. 137 (2001) 261.
[16] P. Carniti, A. Gervasini, A. Auroux, J. Catal. 150 (1994) 274.
[17] P. Carniti, A. Gervasini, A. Auroux, Langmuir 17 (2001) 6938.
[18] D.M. Young, A.D. Crowell, Physical Adsorption of Gases, Butterworth, London, 1962, p. 71.
[19] L.V.C. Rees, D. Shen, in: H. Van Bekkum, E.M. Flamingen, P.A. Jacobs, J.C. Jansen (Eds.), Introduction to Zeolite Science and Practice, Elsevier, Stud. Surf. Sci. Catal. 137 (2001) 579.
[20] J.A. Dunne, R. Mariwala, M. Rao, S. Sircar, R.J. Gorte, A.L. Myers, Langmuir 12 (1996) 5888.
[21] N. Cardona-Martinez, J.A. Dumesic, Adv. Catal. 38 (1992) 149.